

Article

Targeted Substituted-Phenol Production by Strategic Hydrogenolysis of Sugar-Cane Lignin

Danielle Munick de Albuquerque Fragoso¹, Henrique Fonseca Goulart², Antonio Euzebio Goulart Santana² 
and Samuel David Jackson^{1,*} 

¹ Centre for Catalysis Research, School of Chemistry, Joseph Black building, University of Glasgow, Glasgow G12 8QQ, UK; dany.maf2@gmail.com

² Centro de Ciências Agrárias, Universidade Federal de Alagoas, Maceió 57072-900, Alagoas, Brazil; sdj@chem.gla.ac.uk (H.F.G.); aegs@ceca.ufal.br (A.E.G.S.)

* Correspondence: david.jackson@glasgow.ac.uk

Abstract: In this work, a waste-derived lignin with abundant uncondensed linkages, using accessible solvents (acetone/water mixture) and low-cost catalysts showed successful depolymerization for the production of target molecules 4-ethylphenol, 4-propyl-2,6-dimethoxyphenol and 4-propyl-2-methoxyphenol. Lignin samples were obtained from sugar-cane bagasse residue by an organosolv process. Four alumina-based catalysts (Pt/Al₂O₃, Rh/Al₂O₃, Ni/Al₂O₃ and Fe/Al₂O₃) were used to depolymerize the sugar cane lignin (SCL) in an acetone/water mixture 50/50 v/v at 573 K and 20 barg hydrogen. This strategic depolymerisation-hydrogenolysis process resulted in the molecular weight of the SCL being reduced by half while the polydispersity also decreased. Catalysts significantly improved product yield compared to thermolysis. Specific metals directed product distribution and yield, Rh/Al₂O₃ gave the highest overall yield (13%), but Ni/Al₂O₃ showed the highest selectivity to a given product (~32% to 4-ethylphenol). Mechanistic routes were proposed either from lignin fragments or from the main polymer. Catalysts showed evidence of carbon laydown that was specific to the lignin rather than the catalyst. These results showed that control over selectivity could be achievable by appropriate combination of catalyst, lignin and solvent mixture.

Keywords: biomass valorization; lignin; hydrogenolysis; heterogenous catalysis



Citation: de Albuquerque Fragoso, D.M.; Goulart, H.F.; Santana, A.E.G.; Jackson, S.D. Targeted Substituted-Phenol Production by Strategic Hydrogenolysis of Sugar-Cane Lignin. *Biomass* **2021**, *1*, 11–28. <https://doi.org/10.3390/biomass1010002>

Academic Editor: George Z. Papageorgiou

Received: 23 April 2021

Accepted: 10 June 2021

Published: 18 June 2021

Publisher's Note: MDPI stays neutral with regard to jurisdictional claims in published maps and institutional affiliations.



Copyright: © 2021 by the authors. Licensee MDPI, Basel, Switzerland. This article is an open access article distributed under the terms and conditions of the Creative Commons Attribution (CC BY) license (<https://creativecommons.org/licenses/by/4.0/>).

1. Introduction

The interest in repurposing biomass waste has been growing over the years as its effective application can contribute to reduced reliance on fossil fuels [1]. In this context, the chemical structure of lignin is economically attractive in a biorefinery context [2] as it becomes a potential source of value-added molecules [3]. Lignin is an abundant and as yet not defined biopolymer. Its chemical structure varies depending upon the biomass feedstock and extraction method used in its separation from the cell wall network. Generally, three main monomers known as guaiacyl alcohol (G unit), syringyl alcohol (S unit) and *p*-coumaryl alcohol (H unit) [4,5] are considered building blocks of this complex molecule. These units are linked between each other by various linkages, including β -O-4, α -O-4, β - β , 5-5 and β -1 [6].

Lignin can be found in feedstocks such as sawdust, wood chips and sugar-cane bagasse [6,7]. This last one is generated on a large scale (>200 MMT in Brazil) as residue in countries that are producers of bioethanol and sugar, like Brazil, India and China [8]. Most industries use this waste (0.3 T of wet bagasse per tonne sugar cane) in cyclic processes for energy generation [9], however, by using an appropriate pre-treatment it can be an abundant source of lignin (~22% of the dried bagasse). Several approaches have been used to extract lignin from sugar-cane bagasse [10–13]. Alcohols are normally used associated with water in catalytic acidic mediums [14,15]. For the valorization of lignin to fine chemicals, β -O-4 linkages have been shown to be important in depolymerisation [16] and many

researchers have focused on optimizing extraction methods to enhance the quality of the obtained lignin [17]. A suitable metal catalyst with a lignin abundant in β -O-4 bonds could present a promising system for hydrogenolysis with selective production of alkyl-phenolic monomers [16,18]. The methodology behind this is that alkyl-O-aryl bonds can be more readily cleaved compared to C-C bonds (β - β , 5-5 and β -1) in lignin [19]. Selective production of monoaromatics is one of the main challenges regarding depolymerization, due to condensation of intermediates. In general, the lignin is thermally broken, followed by a range of catalytic reactions that lead to phenolics, while the product distribution depends on the catalysts used [18]. Metals such as platinum, rhodium, nickel and iron showed appreciable activity in breaking C-C and C-O-C bonds in model compounds [20–22]. However, when it comes to a real lignin stream, the challenge increases and obtaining selective outcomes becomes harder. Nevertheless, earlier investigations showed that monoaromatics yield can increase in strategic reactions like hydrogenolysis by using metal catalysts [18,23].

One advantage when using acetone in reactions with lignin is this solvent's ability to dissolve the heavier fragments of lignin as previously reported in other studies [18]; thus, contact between lignin and a heterogeneous catalyst can be enhanced. In addition, its commercial production from fermentation of agricultural products has been reported [24], this moves acetone from a petrochemical feedstock to one that is obtainable from renewable sources.

In this work, our investigation focused on a residual-derived lignin with substantial β -O-4 bond content. In spite of considerable information about lignin hydrogenolysis using metal-alumina-based catalysts, there are only a few reports in the literature about compounds that are not generated in the thermolysis (or solvolysis) but exclusively in the catalytic run. Two noble metal catalysts (Pt/Al₂O₃ and Rh/Al₂O₃) and two non-noble metals (Ni/Al₂O₃ and Fe/Al₂O₃) were tested in sugar-cane lignin (SCL) depolymerization. From our observations, target molecules, such as 4-ethylphenol, 4-propyl-2-methoxyphenol and 4-propyl-2,6-dimethoxyphenol could be generated with high selectivity (up to 32%) giving advanced pathways for control in this aspect by using low-cost catalysts and an abundant waste-based lignin with an appropriate solvent mixture. 4-ethylphenol is a fine chemical used for the production of 4-vinylphenol and various antioxidants, which are used in rubber and polymers. It is also an intermediate for pharmaceutical and dye manufacture and is produced on the 500 MT scale annually by a multi-step process. 4-propyl-2,6-dimethoxyphenol is a component of smoked food flavouring, while 4-propyl-2-methoxyphenol is also a food flavouring. Note that even extraction of these components at 1% from sugar cane bagasse lignin residue would satisfy the market for these chemicals and allow the waste material still to be used as a fuel.

2. Experimental

2.1. Catalyst Preparation

A 4.5 wt.% Fe/Al₂O₃ catalyst was prepared by impregnation. Iron nitrate nonahydrate (99%, ACROS Organic) was dissolved in a stoichiometric proportion in deionised water. The metal precursor solution was added to Al₂O₃ (Johnson Matthey, Billingham, Cleveland, UK, pellets size ~5 mm, reference: 961) and the material was left to dry overnight at 313 K. A 4.7 wt.% Ni/Al₂O₃ catalyst was prepared by the highly dispersed catalyst (HDC) methodology as described [25]. Nickel (II) carbonate hydroxide tetrahydrate (98%, Alfa Aesar), ammonium carbonate (NH₃ ca 30%, Alfa Aesar, Heysham, Lancashire, UK) and ammonia water (25% NH₃ bases, Sigma Aldrich, Irvine, Ayrshire Scotland, UK) were used. This methodology consisted in raising the pH in solution in order to promote better catalyst dispersion. Initially, ammonia solution and water were mixed, followed by the addition of ammonium carbonate. The addition of nickel (II) carbonate hydroxide tetrahydrate in the solution resulted in the formation of a nickel amine complex. The solution was slowly added to a round bottom flask containing alumina under stirring. The process was concluded by the evaporation of ammonia in a rotary evaporator. The catalyst was washed with distilled water and left to dry overnight at 323 K. A 1 wt.% Pt/Al₂O₃ catalyst

was obtained commercially from Johnson Matthey (reference number 1074) and a 1 wt.% Rh/Al₂O₃ was prepared by impregnation as previously reported [18].

2.2. Catalyst Reduction

A flow microreactor was used for the reduction of the catalysts. The materials were heated to appropriate reduction temperatures at a ramp rate of 10 K min⁻¹ with a dwell time of 2 h for Pt/Al₂O₃ and 1 h for the other catalysts. The reduction temperature for Pt/Al₂O₃, Rh/Al₂O₃, Ni/Al₂O₃ and Fe/Al₂O₃ was 523 K, 573 K, 850 K and 800 K respectively.

2.3. Sugar-Cane Lignin (SCL) Extraction Process

A straightforward extraction process was used to obtain sugar-cane lignin. Sugar cane bagasse was ground in a laboratory mill (Nogueira type, Itapira, São Paulo) and sieved to 2 mm in a mesh sieve. The bagasse powder was continuously washed with distilled water until it became odorless and dried in an oven at 323 K. 10 g of treated bagasse was added to a 1000 mL round flask with 190 mL of 0.5 M NaOH (VETEC, Rio de Janeiro, RJ, Brazil, class 8) and ethanol (60%, VETEC). The material was heated under reflux at 351 K for 2 h. Subsequently, the reaction mixture was cooled down to room temperature, filtered under vacuum and washed with 500 mL of an ethanol/water 6:4 *v/v* solution. A 1 M HCl (VETEC, class 8) solution was used to acidify the mixture to pH 6 and a volume of ethanol three times the volume of the reaction mixture was added. To separate solid and liquid phases, the material was centrifuged at 10,000 rpm (Rotanta 460 R, Hettich Zentrifugen, Tuttling, Germany) for 10 min. The supernatant was recovered and the solvent was partially removed using a rotary evaporator. A pH of 2 was obtained by adding 1 M HCl solution, followed by the addition of water until the aspect of the solution became opaque. The material was re-centrifuged, the supernatant collected and reserved. The collected material was left to lyophilization for a period of 24 h. The solid dry lignin was used without further procedures.

2.4. SCL Depolymerization Process

A batch autoclave reactor (300 mL) constructed of 316 stainless steel (Parr Instrument Company, Moline, IL, USA) equipped with a digital temperature controller (± 1 K) was used for the depolymerisation experiments. SCL (0.5 g) was added to the reactor with catalyst (0.1 g), with 100 mL of acetone (99.88%, Fisher Scientific, Loughborough, Leicestershire, UK) and distilled water in a 50:50 *v/v* mixture. The reactor was purged with hydrogen three times, pressurised to 20 barg and sealed. The reaction was run at 573 K for 3 h. After reaction, to extract the phenolic compounds generated in the products, the final mixture was filtered using a sintered glass (porosity 3), separating solid residues and catalyst. This liquid material was centrifuged and kept as Fraction 1 (Fraction which contained the fine chemicals). The remained material containing lignin fragments of higher molecular weight was solubilised in 50 mL acetone and kept as Fraction 2. Fraction 1 was acidified to pH 2 using HCl and 0.2 mL of 1g/L hexadecane internal standard added. Products were extracted with dichloromethane (DCM) 3 times, followed by the removal of remaining solvent using a rotary evaporator. After this process, the products were solubilized in 25 mL of DCM.

2.5. Gas Chromatography Mass Spectroscopy Analysis

Product identification and semi-quantification was done as previously reported [26]. A GC-MS QP2010S (Shimadzu, Milton Keynes, Buckinghamshire, UK) coupled to a Shimadzu GC-2010 equipped with a ZB-5MS capillary column (30 m \times 0.25 mm \times 0.25 μ m) with He as carrier was used. The column was kept at 333 K for 2 min then heated to 533 K, where it was held for 10 min. A volume of 1 μ L of sample was injected using split mode (50:1) and an injection temperature of 523 K was used. To improve the analyses, products were deriva-

tized by adding to 10 μL of Fraction 1, 70 μL of *N,O*-bis(trimethylsilyl)trifluoroacetamide (BSTFA) and 30 μL of pyridine. The samples were left for 2 hours prior to injection.

2.6. Product Identification and Yield Calculation

In this initial study of SCL, it was not possible to achieve mass balance closure. All products from Fraction 1 and Fraction 2 could not be identified due to limitations in the extraction method and slight release of gas when the reactor was opened. Hence, it is essential to highlight that the discussion will be centered on the products with higher yield found in the Fraction 1. The estimate of the amount of each product formed was given by the total ion chromatogram (TIC), reference compounds and internal standard. Due to limited commercial availability, four authentic compounds were used as representatives of guaiacyl (G) and syringyl (S) units of lignin. The compounds used were 2-methoxyphenol (Sigma Aldrich, purity 98%), 4-ethyl-2-methoxyphenol (Sigma Aldrich, purity 98%), 2,6-dimethoxyphenol (Sigma Aldrich, purity 99%) and 4-methyl-2,6-dimethoxyphenol (Sigma Aldrich, purity 97%). Calibration using solutions of different concentration (0.01, 0.05, 0.1, 0.5 and 1 g/L) with hexadecane as internal standard (1 g/L) was used to obtain a straight-line graph, where the gradient corresponded to a response factor (α) for each compound. By using α for the correspondent G or S of the chosen reaction product and rearranging Equation (1) by changing reference values per the desired unknown compound values, it was possible to estimate how much it was present in 1 μL . By using Equation (2), considering the total volume of sample (25 mL) and the total amount of lignin used (0.5 g), it was possible to estimate the amount of individual yields in g/100g.

Selectivity was calculated as follows: $S = (\text{the specified molecule} / \text{total amount of detected molecules}) \times 100$. The overall yield was the sum of all fourteen compounds (in g/100g) identified in Fraction 1:

$$\alpha = \frac{\text{Intensity of reference}}{\text{intensity of internal standard}} \times \frac{\text{Mass of internal standard}}{\text{Mass of reference}} \quad (1)$$

$$m \text{ (g/100g)} = \frac{(\text{mass of product from Equation 1} \times 25)}{\frac{0.001}{0.5}} \times 100 \quad (2)$$

2.7. Gel Permeation Chromatography (GPC) and Elemental Analysis (CHN)

GPC analysis was conducted using a Gilson 2 system (Gilson, Dunstable, Bedfordshire, UK), equipped with a UV detector. A set of PS/DVB columns (5 μm , 300 \times 7.5 mm, 50 and 500 \AA , Crawford Scientific Ltd, Strathaven, Lanarkshire, Scotland, UK) was used. The injection volume was 100 μL . The temperature of the column was 303 K. Calibration was conducted with polystyrene standards in the range of 474 to 28,000 g mol^{-1} that were diluted in tetrahydrofuran to 0.5 g L^{-1} . A line equation, $y = -0.031x^3 + 1.2581x^2 - 17.264x + 83.146$, was obtained. Typically, 0.5 g of lignin or reaction product (prepared by combining equal volumes of Fraction 1 and Fraction 2, followed by solvent evaporation) were acetylated with 0.5 mL of pyridine and 0.5 mL of acetic anhydride overnight. After solvents removal by N_2 blowing, the sample was completely solubilized in THF prior to injection. The ChromPerfect software package was used to manage the data. CHN analysis was carried out on a CE-440 Elemental Analyser (Exeter Analytical (UK), Ltd, Coventry, Warwickshire, UK).

2.8. Thermogravimetric Analysis (TGA)

The temperature programmed oxidation analysis (TPO) was performed using a combined TGA/DSC SDT Q600 thermal analyser (TA instruments UK, Elstree, Hertfordshire, UK) coupled to an ESS mass spectrometer. About 0.01–0.015 g of catalyst was used and the samples were heated from room temperature to 1273 K with a thermal ramp of 10 K min^{-1} under O_2/Ar .

2.9. Surface Area and Pore Volume Determination (BET)

A Gemini III 2375 Surface Area analyser (Micrometrics, Hexton, Hertfordshire, UK) was used. About 0.04 g of catalyst sample was added to a glass tube and left overnight at 383 K under nitrogen. The samples were reweighed prior to analysis at 77 K.

2.10. Raman and Atomic Absorption Spectroscopy Analysis

A LabRAM High resolution spectrometer (Horiba Jobin Yvon, Glasgow, Lanarkshire, Scotland, UK) was used in this analysis. Helium cadmium IK3201 and R-F 325 nm UV lasers were used. The laser light was directed to the sample for 10 seconds using a $15 \times$ UV objective lens with 1200 cm^{-1} grating. A range of 500 to 3000 cm^{-1} was used. Back scattering configuration collected the scattered light and detected by a nitrogen cooled charge-coupled detector CCD. For atomic absorption spectroscopy analysis a Perkin Elmer analyst 400 atomic absorption spectrometer, equipped with winlab 32 was used.

3. Results and Discussion

3.1. Catalyst Characterization

Pt/Al₂O₃, Rh/Al₂O₃, Ni/Al₂O₃ and Fe/Al₂O₃ were characterized using a range of techniques. Atomic absorption spectroscopy gave metal loadings of 4.7 wt% for Ni and 4.5 wt% for Fe supported on alumina, while BET analysis for Ni/Al₂O₃ gave a surface area of $106 \text{ m}^2 \text{ g}^{-1}$, pore volume of $0.5 \text{ cm}^3 \text{ g}^{-1}$ and a pore diameter of 12.6 nm, and for Fe/Al₂O₃ a surface area of $90 \text{ m}^2 \text{ g}^{-1}$, pore volume of $0.4 \text{ cm}^3 \text{ g}^{-1}$ and a pore diameter of 145 nm. X-ray diffraction analysis revealed that these catalysts' support was mostly composed of theta- and delta-alumina. As previously reported [18], 1% Pt/Al₂O₃ was obtained commercially by Johnson Matthey (reference number 1074). XRD analysis showed that the support was mainly θ -alumina. BET analysis gave a surface area of $124 \text{ m}^2 \cdot \text{g}^{-1}$, a pore volume of $0.6 \text{ cm}^3 \cdot \text{g}^{-1}$ and a pore diameter of 14.6 nm. Carbon monoxide chemisorption analysis gave a dispersion of 56% and hence an average particle size of $\sim 2 \text{ nm}$ [18]. 1 wt.% Rh/Al₂O₃ was prepared by impregnation [18], having a surface area of $102 \text{ m}^2 \cdot \text{g}^{-1}$, a pore volume of $0.5 \text{ cm}^3 \cdot \text{g}^{-1}$ and a pore diameter of 14.5 nm, as measured by BET. While carbon monoxide chemisorption gave a dispersion of 121% [18] and XRD showed that the support was composed by θ - and δ -alumina [18].

3.2. Sugar-Cane Lignin (SCL) Characterization

3.2.1. Elemental Analysis

Elemental analysis of the SCL reported in Table 1 gave an approximate chemical formula of C₉H₁₁O₅, which would not be inconsistent with SCL lignin having a mixture of H, G and S units [27] and an O/C ratio of 0.55. This oxygen content was in line with catalytic results, which suggested more syringyl units and an appreciable degree of alkyl-ether linkages.

Table 1. Elemental analysis of SCL (oxygen content was estimated by difference).

Elemental Analysis (%)	
C	54.1
H	5.6
N	0.9
O	39.4

3.2.2. Molecular Weight Distribution of SCL

GPC analysis gave an overview of the mass distribution, molecular number and polydispersity of SCL and depolymerisation products by analysis of combined Fraction 1 (fraction which contained the fine chemicals) and Fraction 2 (acetone soluble residual lignin). As the samples were mixtures, there were variations in the UV response and limitations to be able to associate peaks with specific molecules. Figure 1 shows typical

GPC profiles of SCL, acetone reference reaction (catalyst free, reference reaction with solvent 50/50 acetone/water) and a Pt/Al₂O₃ catalysed reaction. Compared to the initial lignin, there was a shift to lower molecular weight products. Hence, the abundant condensed fraction at about 12 min in SCL disappeared, giving a lower-Mw broad peak eluting at ~ 13–15 min. Overall, the reference and the catalyzed experiments showed very similar GPC profiles, however, in the presence of Pt/Al₂O₃ there was a gain of relative intensity in the lower molecular weight GPC peak, indicating larger uncondensed fractions from the catalyzed experiments. Confirming these findings, the molecular weight decreased from 2291 Da (SCL) to 1355 Da for the uncatalyzed reference reaction and ~1179 Da for catalyzed reactions. The molecular number also decreased (731 for SCL, 541 for the reference and 517 for catalyzed) as there was conversion of macromolecules into others [28]. The decrease in the polydispersity (3 for SCL, 2.5 for reference and 2.3 for catalyzed) showed the presence of less complex and branched molecules compared to the initial lignin. Hence, although lignin degradation occurred for thermolysis, it was more efficient with the presence of a catalyst.

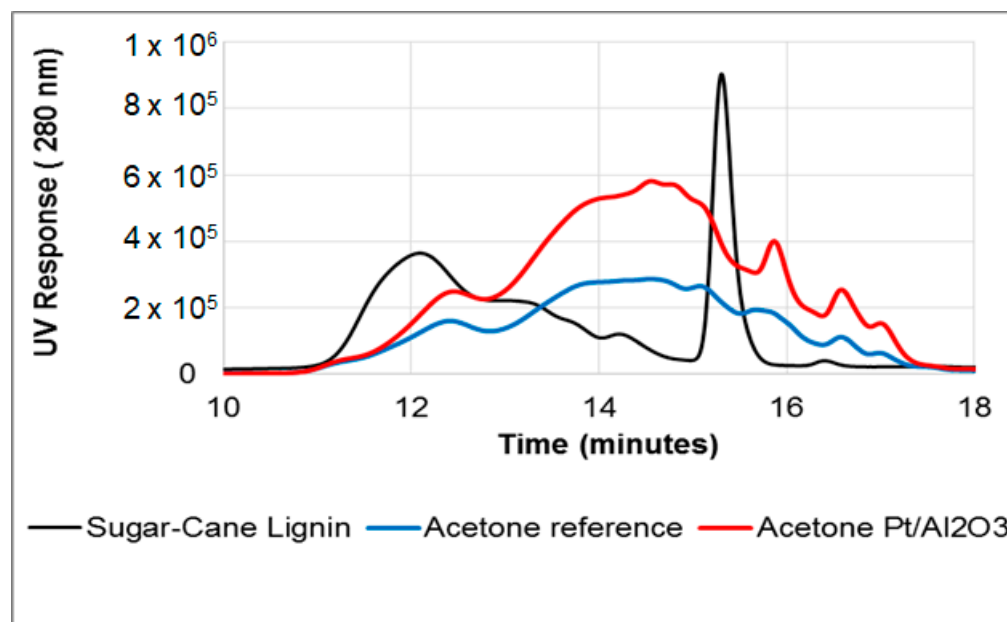


Figure 1. GPC profile of SCL, reference and Pt/Al₂O₃ catalysed reactions.

3.2.3. Product Distribution and Quantification by GC/MS

After the experiment, the extracted fraction containing lighter molecules (Fraction 1) was analyzed via GC/MS. The standard deviation (SD) for individual monoaromatics' yield (g/100g) was determined from triplicates carried out in our earlier investigations [26,29], the SD values were below 0.1, which was deemed an acceptable range. Fourteen molecules from SCL depolymerization were identified and are listed in Table 2. They were, in general, alkylated molecules, and there was a considerable difference in syringyl-yield/guaiacyl-yield ratio with more S unit-type of products. Note this methodology did not identify hydrogenated or cyclohexanol molecules. According to the type of products, deoxygenation was also assumed to occur, this could be in more than one step or directly by C-O or alkyl chain breakdown. This analytical method was used to semi-quantify individual product yield, with response factors calculated based on lignin model molecules: the values used for compounds derived from a G or S unit were 0.23 and 0.19, respectively.

Table 2. Identified compounds from SC lignin depolymerisation.

Compound Code	Compound Name
(1)	2-methoxyphenol
(2)	4-methyl-2-methoxyphenol
(2A)	4-ethylphenol
(3)	4-ethyl-2-methoxyphenol
(4)	4-propyl-2-methoxyphenol
(5)	1,2-dihydroxybenzene
(6)	4-ethylbenzene-1,2-diol
(6A)	2,6-dimethoxyphenol
(7)	4-(3-hydroxypropyl)-2-methoxyphenol
(8)	4-(3-methoxypropyl)-2-methoxyphenol
(9)	4-methyl-2,6-dimethoxyphenol
(10)	4-(2-hydroxyethyl)-2,6-dimethoxyphenol
(11)	4-ethyl-2,6-dimethoxyphenol
(12)	4-propenyl-2,6-dimethoxyphenol
(13)	4-(2-hydroxyethyl)-2-methoxyphenol
(14)	4-propyl-2,6-dimethoxyphenol
(15)	4-(1-hydroxy-2-methylpent-3-enyl)-2,6-dimethoxyphenol
(15A)	4-(3-hydroxypropyl)-2,6-dimethoxyphenol

3.2.4. Depolymerisation of Sugar-Cane Lignin (SCL)

Efficient depolymerisation of lignin remains challenging and one strategy to address this issue is the use of less recalcitrant (uncondensed) lignins, as higher yields of monoaromatics have been reported from catalytic depolymerization of these substrates [16–18]. This could be achieved by a suitable pre-treatment in the extraction step, resulting in a biopolymer richer in alkyl-O-aryl-type of linkages. In a biorefinery context [5,30], this is a relevant strategy as it is based on sustainable production of platform chemicals from waste. In this study, an approach of using a less condensed sugar-cane lignin, an authentic biomass-derived material, was used to obtain value-added chemicals. Experiments aiming selective rupture of aryl-ether bonds such as β -O-4 and β -O-4 (Et) from SCL molecular framework, involved Pt/alumina, Rh/alumina, Ni/alumina and Fe/alumina catalysts; as will be further discussed, an increase in product yield and promising catalytic activity was found.

3.2.5. Catalyst Free System

Control tests (573 K, 20 barg H₂, solvent, acetone/water 50:50 *v/v*) on SCL depolymerization were conducted. Monoaromatics have been formed from lignin solvolysis mostly using alcohol [18,31] water [32] and various solvent mixtures [26,33]. In addition, kinetic isotopic effects recently showed that an acetone/water mix was directly involved in product formation from Kraft lignin, in both non-catalytic and catalytic runs [26]. Nevertheless, as shown in Figure 2, catalyst free experiments (reference) showed a low overall yield of 3.9 g/100 g composed mainly of phenolics with alkyl chains attached to the α -carbon from syringyl and guaiacyl units. Product distribution showed depletion of linkages by thermolysis, however, the low yields associated with solvolysis leads to high re-polymerisation issues and lack of selectivity.

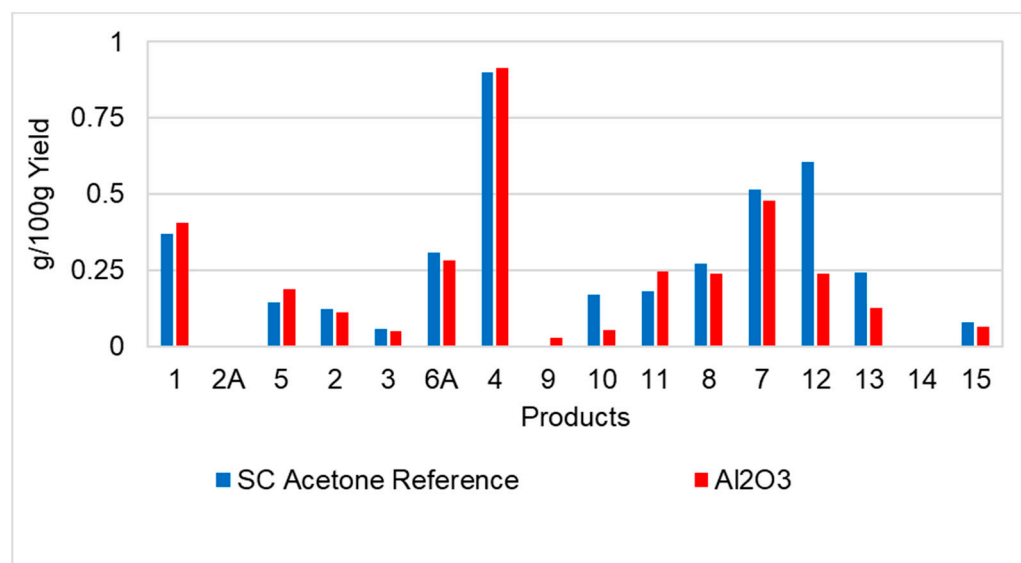


Figure 2. Estimated yield in g/100g of phenolic compounds in solvolysis (reference) and reactions in the presence of Al₂O₃ support. Standard deviation value: 0.1. Products identified by GC-MS: (1) 2-methoxyphenol, (2) 4-methyl-2-methoxyphenol, (2A) 4-ethylphenol, (3) 4-ethyl-2-methoxyphenol, (4) 4-propyl-2-methoxyphenol, (5) 1,2-dihydroxybenzene, (6A) 2,6-dimethoxyphenol, (7) 4-(3-hydroxypropyl)-2-methoxyphenol, (8) 4-(3-methoxypropyl)-2-methoxyphenol, (9) 4-methyl-2,6-dimethoxyphenol, (10) 4-(2-hydroxyethyl)-2,6-dimethoxyphenol, (11) 4-ethyl-2,6-dimethoxyphenol, (12) 4-propenyl-2,6-dimethoxyphenol, (13) 4-(2-hydroxyethyl)-2-methoxyphenol, (14) 4-propyl-2,6-dimethoxyphenol, (15) 4-(1-hydroxy-2-methyl-pent-3-enyl)-2,6-dimethoxyphenol. Conditions: 573 K, 20 barg H₂, solvent, acetone/water 50:50 *v/v*.

3.2.6. Effect of Alumina Support

Tests with Al₂O₃ investigated its stability and whether the support would have an influence on SCL degradation. Experiments were carried out with Al₂O₃ while the other reaction parameters were kept the same. Alumina is involved in many industrial processes due to its high surface area but also high catalytic surface activity. It has activity in ethanol and isopropanol conversion [34], alcohol dehydration [35] and H-H, C-H and C-C bonds activation [36], indicating the possibility of an effect in the breakdown of SCL chemical structure. Al₂O₃ with acetone/water gave a poor performance (Figure 2). The reason behind this may be associated to the high concentration of acetone. Reactivity of this solvent was reported on the surface of alumina with its adsorption on the Lewis acidic sites [37] and, when compared to zeolites, acetone activation was found to be faster with alumina [37]. Thus, competitive reactions on alumina surface between acetone and lignin fragments could occur, decreasing this solvent capacity in dissolving lignin and availability of alumina Lewis-Bronsted acid sites to acid-base reactions. Nevertheless, alumina showed some degree of catalytic activity, compared to solvolysis, with yields of compounds 1, 4, 5 and 11 slightly increased, and detection of a new compound, 4-methyl-2,6-dimethoxyphenol (9), as shown in Figure 2. However, overall yield was 3.4 g/100 g, with alumina mostly promoting condensation reactions as has been reported [38]. Thus, solvolysis and experiments with Al₂O₃ were comparably ineffective, giving a similar extent of SCL degradation and high lignin re-condensation.

3.2.7. Catalysts Screening

Pt/Al₂O₃, Rh/Al₂O₃, Ni/Al₂O₃ and Fe/Al₂O₃ were compared under the same reaction conditions. Overall monophenolic yield for Pt-, Rh-, Ni- and Fe/alumina was 11.4%, 12.9%, 8.3% and 6.6%, respectively, without ring-hydrogenation activities. These values, up to three times higher compared to thermolysis and Al₂O₃ tests, revealed substantial catalyst chemoselectivity. The negligible contribution from thermolysis or alumina allows

the assignment of the reaction specificity to the metal. At the studied conditions, acetone was at a high enough temperature and pressure to reach the supercritical state (SC) [39], though this is not the case for ${}_{sc}\text{H}_2\text{O}$ [40]. Conditions to reach supercritical fluid in the reaction could be affected due to intermolecular interactions between the solvents as they were mixed (acetone/water 50:50 *v/v*). Still, variations in dielectric constants giving higher lignin fragment solubility and stabilization were expected [40]. These aforementioned characteristics, enhancement of hydrogen diffusion, and the presence of heterogenous catalysts could be among the combined factors associated with improvement in product formation. Detailed results of each catalyst's monophenolics yield and distribution is discussed in the following sections.

3.2.8. Effect of Pt and Rh Noble Metal Catalysts

From Figure 3 it can be seen that most products increased in yield by the addition of these catalysts. Distribution of guaiacyl and syringyl derived molecules were well balanced, with higher yields for S unit-products due to the nature of the starting lignin. The main products were 4-ethylphenol (2A) and 2,6-dimethoxyphenol (6A), with selectivities of ~28% and ~15% for Pt and ~20% and ~15% for Rh, respectively. These molecules highlighted similarities in these catalysts' ability to catalyse dealkylation and deoxygenation, especially Pt/ Al_2O_3 . In Figure 3, it is relevant to note that Pt increased the yield mainly of products 2A, 6A, 11 and 14 whereas Rh increased the yield more generally for most of the products. Thus, despite rhodium effectiveness, Pt was indeed more selective. Similarly, in experiments with an ammonia derived lignin [18] even with Pt and Rh giving similar selectivity towards alkylphenolics, Rh was suggested, in general, as more effective in cleaving alkyl-aryl linkages. This behaviour of higher selectivity for Pt with SCL, when compared to ammonia lignin, could lead to the association of selectivity not only to the metal, but also to the less condensed nature of a lignin.

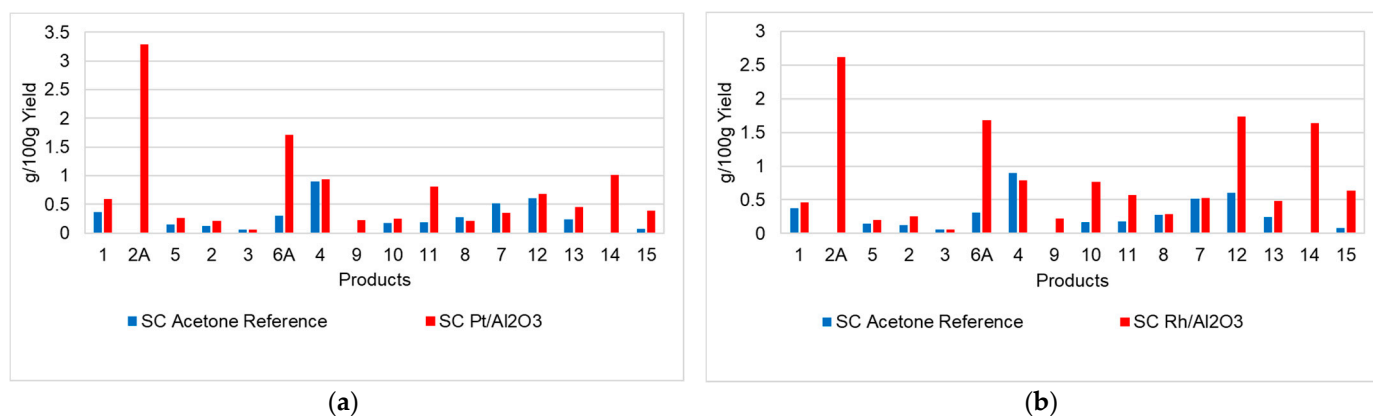


Figure 3. Estimated yield in g/100g of phenolic compounds in solvolysis (reference), reactions in the presence of (a) Pt/ Al_2O_3 and (b) Rh/ Al_2O_3 catalysts. Standard deviation value: 01. Products identified by GC-MS: (1) 2-methoxyphenol, (2) 4-methyl-2-methoxyphenol, (2A) 4-ethylphenol, (3) 4-ethyl-2-methoxyphenol, (4) 4-propyl-2-methoxyphenol, (5) 1,2-dihydroxybenzene, (6A) 2,6-dimethoxyphenol, (7) 4-(3-hydroxypropyl)-2-methoxyphenol, (8) 4-(3-methoxypropyl)-2-methoxyphenol, (9) 4-methyl-2,6-dimethoxyphenol, (10) 4-(2-hydroxyethyl)-2,6-dimethoxyphenol, (11) 4-ethyl-2,6-dimethoxyphenol, (12) 4-propenyl-2,6-dimethoxyphenol, (13) 4-(2-hydroxyethyl)-2-methoxyphenol, (14) 4-propyl-2,6-dimethoxyphenol, (15) 4-(1-hydroxy-2-methyl-pent-3-enyl)-2,6-dimethoxyphenol. Conditions: 573 K, 20 barg H_2 , solvent, acetone/water 50:50 *v/v*.

These variations found with Rh and Pt were evidenced also in other studies. Bouxin and co-authors in their study of hydrodeoxygenation of *p*-methylguaiacol found different main products from these metals - platinum with greater selectivity to 4-methylcatechol while rhodium gave cresols [41]. An investigation of the use of these metals to produce biobased chemicals from Kraft lignin [42] showed best results by Rh, with 30 wt% of monomer yield. In addition, when studying bibenzyl model compound, Yamaguchi et al.

found an effective C-C cleavage by Rh [20]. Thus, rhodium was expected to give higher overall yield.

Regarding lignin-type linkages, these metals can be involved in more than one reaction during depolymerisation [43]. For example, hydrogenolysis and hydrolysis were found as essential to the rupture of C-O in studies with $scCO_2$ /water, Rh/C and diphenyl ether [44]. This is relevant considering the lignin complexity and the several steps to finally result in monophenolics from this biopolymer [23]. For SCL experiments, we found Pt selective, but Rh had a higher extent of C-C and C-O-C bond rupture, inferring greater intermediates stabilization by rhodium.

3.2.9. Effect of Ni and Fe Catalysts

Depolymerisation of SCL with Ni/Al₂O₃ and Fe/Al₂O₃ gave different selectivity plots compared to the noble metals (Figure 4). Both had higher yields towards one specific compound, 4-ethylphenol (2A), followed by 2-methoxyphenol (1) and 4-ethyl-2,6-dimethoxyphenol (11). Other main products for Ni were 2,6-dimethoxyphenol (6A) and 4-propyl-2,6-dimethoxyphenol and for Fe 4-ethyl-2-methoxyphenol (3) and 4-(2-hydroxyethyl)-2,6-dimethoxyphenol (10). Overall, according to Figure 4, if the desired reaction was dealkylation, nickel was appropriate, whereas iron would mainly give branched type of products. SCL depolymerisation using nickel showed a consistent level of selectivity, with highest yield for 2,6-dimethoxyphenol and 4-ethylphenol. The catalytic activity of these metals was not a surprise. In the literature, studies with model compounds using nickel and iron gave a variety of products [22,23], thus, it would be surprising if it were to be different with a real lignin in reaction with these metals. Song and co-authors demonstrated depolymerisation of a birch derived lignin through alcoholysis followed by hydrogenolysis using a nickel catalyst [23]. An α -O-4 bond in benzyl phenyl ether was cleaved by hydrolysis without catalyst, however, once a nickel catalyst was added, the predominant route was hydrogenolysis [45]. Interestingly, Jiayue et al. reported bond cleavage on the Ni surface as the rate determining step in the hydrogenolysis of a 4-O-5 bond [46]. We found that with a real SCL, hydrogenolysis and deoxygenation were also appreciable when using a nickel-based catalyst. For iron [22], rupture of linkages such as α -O-4 and β -O-4 gave toluene and phenol. These authors [22] also found relevance in the position of -OH group regarding to the β -O-4-type molecule, thus, the groups around the linkages that were cleaved influenced how a reaction proceeds. When Yoshikawa et al. investigated a two-step process of phenol production from lignin, they reported that iron oxide favoured catechol and methoxyphenol conversion to molecules like phenols, cresols and alkylphenols [47]. Many reactions like hydrogenolysis, hydrodeoxygenation, hydrogenation, dehydration, decarboxylation, and decarbonylation [43,48] can occur in lignin depolymerisation and the final product depends upon the type of catalyst used.

The findings in this work were not divergent to this aspect, iron and nickel had different product distributions, nevertheless, our studies showed that compared to noble metals (Rh and Pt), it was possible to achieve appreciable product yields for the reductive catalytic hydrogenolysis using lower cost catalysts.

3.2.10. Catalytic Products

Three molecules were detected in the catalytic experiments and identified as follows: 4-ethylphenol (2A), 4-methyl-2,6-dimethoxyphenol (9) and 4-propyl-2,6-dimethoxyphenol (14). These were not simple thermal products but came from effective catalytic activity.

Figure 5 presents the selectivity values according to the catalyst used. As regards product 9, there were similar yields for all. Alumina's acidic sites can catalyse hydrolysis and alkylation [45], thus, this product formation, first detected in reaction with only alumina (Figure 2), was associated with the Al₂O₃ support with no relevant influence of the metals.

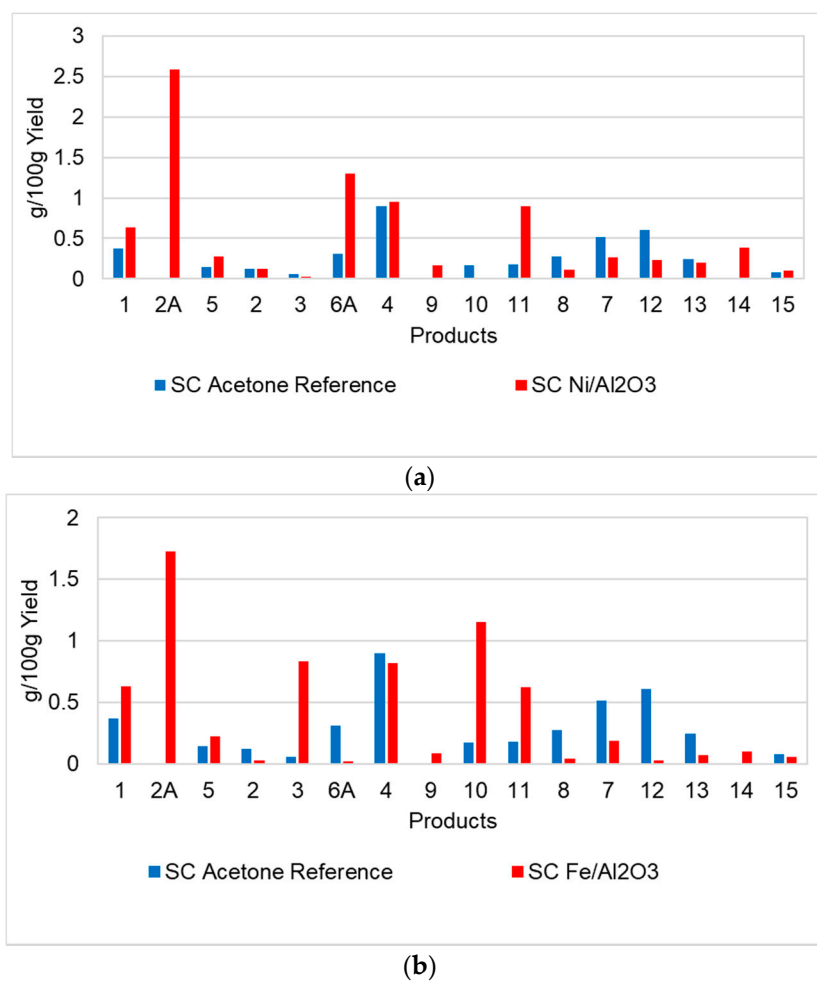


Figure 4. Estimated yield in g/100g of phenolic compounds in solvolysis (reference), reactions in the presence of (a) Ni/Al₂O₃ and (b) Fe/Al₂O₃ catalysts. Standard deviation value: 0.1. Products identified by GC-MS: (1) 2-methoxyphenol, (2) 4-methyl-2-methoxyphenol, (2A) 4-ethylphenol, (3) 4-ethyl-2-methoxyphenol, (4) 4-propyl-2-methoxyphenol, (5) 1,2-dihydroxybenzene, (6A) 2,6-dimethoxyphenol, (7) 4-(3-hydroxypropyl)-2-methoxyphenol, (8) 4-(3-methoxypropyl)-2-methoxyphenol, (9) 4-methyl-2,6-dimethoxyphenol, (10) 4-(2-hydroxyethyl)-2,6-dimethoxyphenol, (11) 4-ethyl-2,6-dimethoxyphenol, (12) 4-propenyl-2,6-dimethoxyphenol, (13) 4-(2-hydroxyethyl)-2-methoxyphenol, (14) 4-propyl-2,6-dimethoxyphenol, (15) 4-(1-hydroxy-2-methyl-pent-3-enyl)-2,6-dimethoxyphenol. Conditions: 573 K, 20 barg H₂, solvent, acetone/water 50:50 *v/v*.

Once in the presence of metals, major yield differences were observed between compounds 2A and 14. For 4-propyl-2,6-dimethoxyphenol (14), its generation may be in line with the ability of each catalyst to cleave β -O-4 bonds, as propyl side chain products are usually generated from this type of linkage rupture [49]. This ability increased as follows: Rh > Pt > Ni > Fe. Previously [27], temperature programmed reduction (TPR) analysis showed that uncondensed lignins degraded into smaller fragments in a range < 573 K. As confirmed by solvolysis, SCL fragmentation also started without the need of a catalyst. Considering SCL intermediates having ether bonds (β -O-4) present in this mild temperature process (573 K), and a hydrogen rich environment with suitable catalyst's metal sites for its dissociative adsorption, a similar cleavage pathway to selective thioacidolysis [49] could occur. This could initiate with lignin fragmentation, followed by hydrogenolysis of C_{alkyl}-O bond of β -O-4 containing intermediates and stabilisation by the intake of a hydrogen atom at the unstable alkyl chain carbon, finally leading to the formation of a product such as 4-propyl-2,6-dimethoxyphenol. In this instance, Rh/Al₂O₃ was the most efficient catalyst.

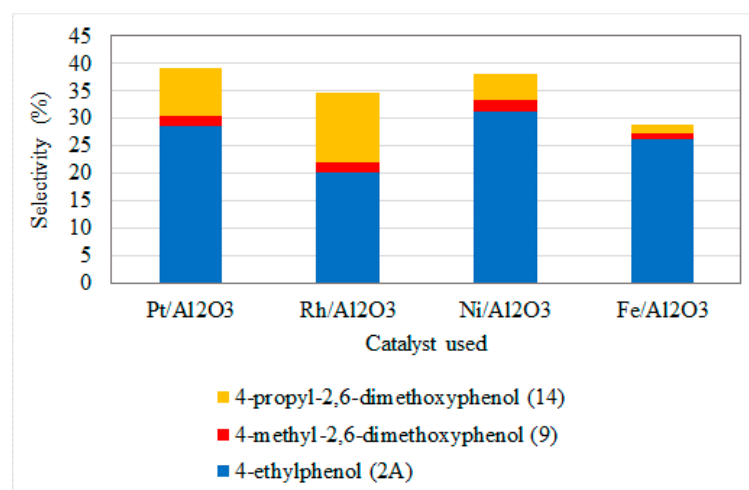


Figure 5. Selectivity of compounds 4-ethylphenol (2A), 4-methyl-2,6-dimethoxyphenol (9), and 4-propyl-2,6-dimethoxyphenol (14) between the four alumina catalysts.

Regarding 4-ethylphenol (2A), while platinum and rhodium catalysts selectively produced ~20% and 28%, nickel and iron gave ~31% and ~26%, respectively. It is important to note that nickel, a non-noble metal, had as good a catalytic effect as the noble metals. Two potential reaction pathways to generate 4-ethylphenol are suggested. First (Figure 6a), as the yield of 4-ethyl-2-methoxyphenol (3) dropped in the catalytic runs compared to solvolysis (Figure 3), 4-ethylphenol could come from simple catalytic demethoxylation of compound 3.

Another route (Scheme 1B) could be related to the chemical structure of SCL, if a *p*-coumaryl alcohol-type fragment was derived from SCL depolymerisation, (i) hydrogenolysis could occur in the presence of a heterogenous catalyst, followed by (ii) decarboxylation giving a 4-vinylphenol-type species as an intermediate, which by (iii) hydrogenation would result in 4-ethylphenol.

The solvent mixture could also play a key role in the depolymerisation. Hydrolysis was likely to occur enhancing lignin cracking [50] and acetone can dissolve lignin heavier fragments [18]. Moreover, at this temperature and pressure, water can interact with organic molecules and the presence of OH⁻ and H⁺ favours acid/base catalysed reactions [40]. Various approaches with lignin solvolysis have been proposed [12,26,43]. Kraft and organosolv lignins were shown to depolymerise with supercritical acetone and alumina based catalysts [51] and Erdocia and co-authors described that when a range of lignins were treated with ^{sc}methanol, ^{sc}ethanol and ^{sc}acetone, this last solvent was shown to be the best, giving higher oil yield; water was also shown to be more effective when mixed with another solvent promoting decomposition of lignin [52]. Although there are these effects from solvolysis, greater conversion of SCL was significantly dependent upon the catalysts used. The combination of solvent mixture along with appropriate catalyst resulted in higher overall yield (for Rh/Al₂O₃) and efficient target molecule generation, especially non-alkylated monophenols (for Ni/Al₂O₃). Differences between catalysts should be expected due to the number of different reactions (Scheme 1) often occurring on different active sites. For example, hydrogenolysis is highly structure sensitive, whereas aromatic hydrogenation is much less so and both will use different sites. However this gives the potential for more selective behaviour.

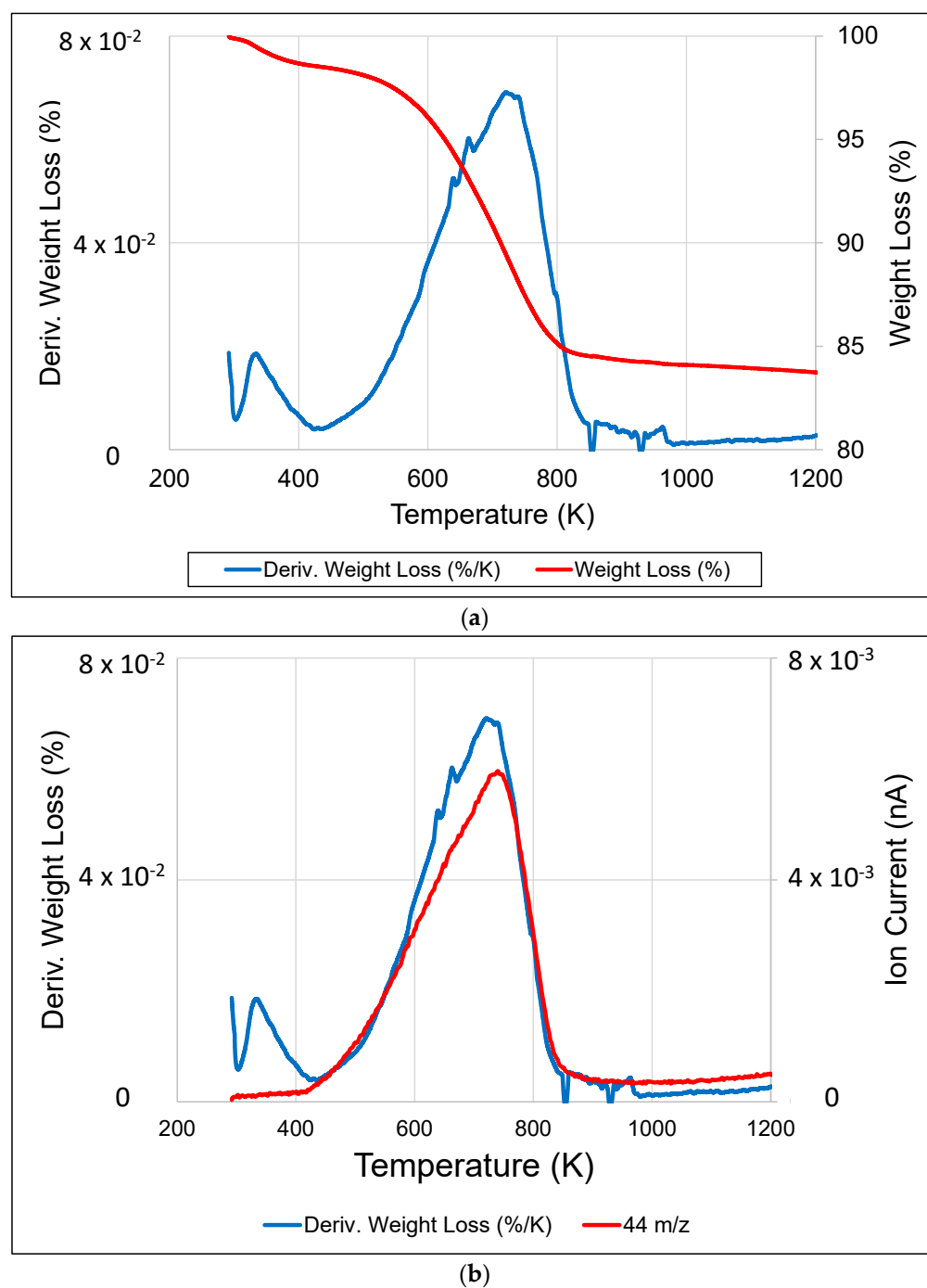
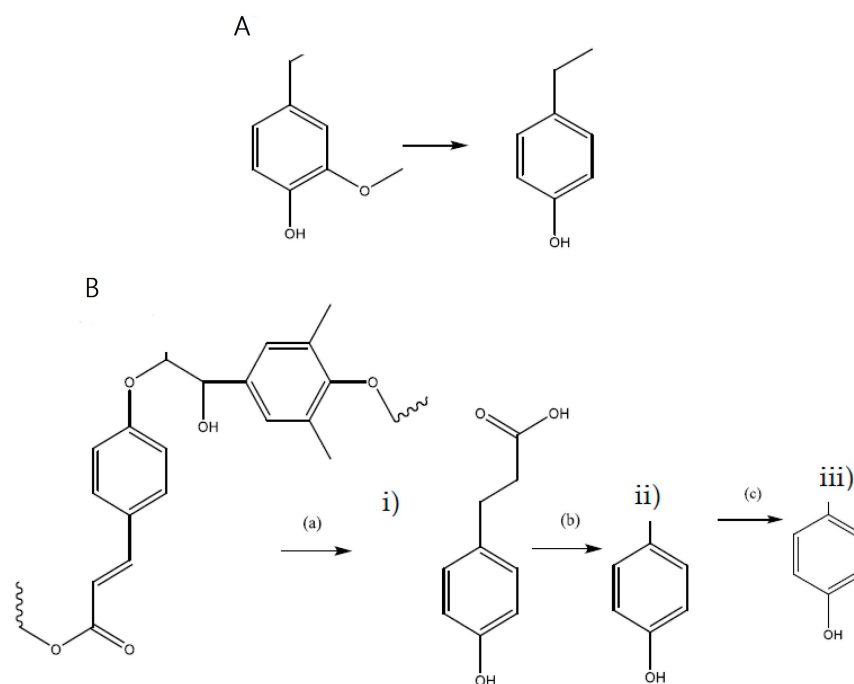


Figure 6. TPO of spent Pt/Al₂O₃ catalysts after acetone/H₂O reaction with the sugar-cane lignin. (a) weight loss and derivative weight loss as a function of temperature, (b) evolution of CO₂, as evidenced by the increase of m/z 44, as a function of temperature mapping on to the derivative weight loss.



Scheme 1. Possible reaction pathways for the formation of 4-ethylphenol. (A) Catalytic demethoxylation of 4-ethyl-2-methoxyphenol resulting in 4-ethylphenol, (B) (i) hydrogenolysis of a *p*-coumaryl alcohol lignin fragment (ii) decarboxylation and formation of 4-vinylphenol-type specie as intermediate, (iii) hydrogenation resulting in 4-ethylphenol.

An ideal type of lignin and a physical, chemical or biocatalytic processes to generate fine chemicals is yet not established. For effective lignin hydrogenolysis, a combination of factors must be addressed, such as viability of the substrate (usually controlled by feedstock), the type of extraction process, depolymerisation-condensation balance, solvent and catalyst. In this work, it was decided to extend to SCL previous optimisation conditions found for ammonia-derived lignin [18]. Indeed, catalytic products from SCL could be successfully obtained at these conditions and the studied catalysts, giving overall yields up to ~ 3 times higher than thermolysis, however, condensation could not be fully overcome. It was interesting to make this comparison because, in contrast to ammonia lignin [18] and SCL, tests with a Kraft lignin [26] using these same reaction conditions showed no significant effect of catalysts compared to solvolysis, which may be associated to its recalcitrant degree of condensation (C-C type of bonds), thus, reinforcing the applicability of lignin structure in hydrogenolysis strategies. Yet, despite of promising results, each lignin behaved as a unique system and SCL required its own optimisation to give it its full potential. Overall, this extracted raw substrate had appreciable activity for hydrogenolysis, providing specific monophenolics only in catalytic tests and according to the type of metal, giving selectivity up to 32% for 4-ethylphenol using Ni/Al₂O₃. Most importantly, the results indicated that control upon selectivity is possible by using an appropriate lignin, catalyst and solvent mixture.

4. Post-Reaction Catalyst Evaluation

Stability of alumina in the presence of water at high pressure and temperature could be affected by hydration and Al₂O₃ phase transition. This has been found [53] in studies with γ -alumina undergoing transformations to boehmite at 473 K. Here, θ -alumina, which is considered more stable [18] was used, nevertheless it was of interest to investigate whether chemical or physical changes occurred with the catalysts. Elemental analysis of post-reaction Al₂O₃, Pt/Al₂O₃ and Ni/Al₂O₃ revealed that there was carbon laydown but also traces of hydrogen and nitrogen (Table S1, Supplementary Materials), confirming

the interaction of lignin and catalyst during the reaction. Following these results, TPO analysis (Figure 6) also showed the presence of carbonaceous deposits. It is noticeable that compared to Al_2O_3 (Figure S1, Supplementary Materials), the metal catalysts had a higher mass loss (~15%) which would be expected if the carbon deposit was associated with enhanced interaction between lignin and metal-support system. Looking in detail at the TPO plots (Figure S1, Figure S2, Supplementary Materials), there was a similar profile for all catalysts with an initial weight loss at 250 K–380 K, associated with physisorbed water. Subsequently, a main weight loss between ~400 K and 800 K, which was related to CO_2 evolution, as shown in Figure 6. At this temperature, the adsorbed species could be pseudo-molecular [41]. There were small events below 700 K for all catalysts indicating more than one type of carbonaceous deposit. As no further weight loss was observed above 800 K, no recalcitrant species were present on the surface. In agreement with these results, Raman spectroscopy revealed (Figure S3, Supplementary Materials) low intensities of disordered and graphitic bands in the used catalysts. They were associated to D and G bands [54,55] at $\sim 1380\text{ cm}^{-1}$ and $\sim 1600\text{ cm}^{-1}$, respectively and the D/G ratio of 0.1 suggested that there was more slightly ordered carbon species in nature. Previous studies using Al_2O_3 and $\text{Pt}/\text{Al}_2\text{O}_3$ at the same reaction conditions of this study (with Kraft lignin) gave no modification in the support's XRD patterns after reaction [26]. This stability could be associated to a synergistic effect between the metals and the support [54] preventing phase transition and the presence of oxygenates in the reaction medium, interacting with the alumina surface, inhibiting hydrolysis. Finally, BET analysis (Table S2, Supplementary Materials) revealed an increase in the surface area and decrease of pore volume due to the deposit of carbon species.

5. Conclusions

In this work, a waste-derived lignin with abundant uncondensed linkages, using accessible solvents (acetone/water mixture) and low-cost catalysts showed successful depolymerization with the generation of the target molecules 4-ethylphenol, 4-propyl-2,6-dimethoxyphenol and 4-propyl-2-methoxyphenol. Lignin was extracted from sugar cane bagasse and depolymerized in the presence of a series of catalysts at 573 K, 20 barg H_2 , with solvent, acetone/water 50:50 *v/v*. The molecular weight of the lignin was reduced by half by the catalytic reaction and the polydispersity also decreased showing the presence of less complex and branched molecules compared to the initial lignin. Specific metals directed product distribution and yield, with $\text{Rh}/\text{Al}_2\text{O}_3$ having the greatest overall yield, but with $\text{Ni}/\text{Al}_2\text{O}_3$ showing the highest selectivity to a given product (~32% to 4-ethylphenol). Mechanistic routes were proposed either from lignin fragments or from the main polymer. Catalysts showed evidence of carbon laydown that was specific to the lignin rather than the catalyst.

Supplementary Materials: The following are available online at <https://www.mdpi.com/article/10.3390/biomass1010002/s1>, Figure S1 TPO plot (left) and derivative weight loss (right) with CO_2 m/z 44 evolution of spent Al_2O_3 catalyst after acetone/ H_2O reaction with the sugar-cane lignin, Figure S2 TPO plot (left) and derivative weight loss (right) with CO_2 m/z 44 evolution of spent $\text{Ni}/\text{Al}_2\text{O}_3$ catalyst after acetone/ H_2O reaction with the sugar-cane lignin, Table S1 Elemental analysis of spent alumina catalysts in SCL depolymerisation, Raman spectrum of spent Al_2O_3 support, $\text{Pt}/\text{Al}_2\text{O}_3$ and $\text{Ni}/\text{Al}_2\text{O}_3$, Table S2 BET analysis of spent Al_2O_3 , $\text{Pt}/\text{Al}_2\text{O}_3$ and $\text{Ni}/\text{Al}_2\text{O}_3$.

Author Contributions: D.M.d.A.F.: Funding acquisition, Validation, Formal analysis, Investigation, Writing—original draft, Writing—review & editing. H.F.G. Investigation, Formal analysis. A.E.G.S.: Investigation, Formal analysis. S.D.J.: Supervision, Project administration, Writing—review & editing. All authors have read and agreed to the published version of the manuscript.

Funding: This research was funded by the Conselho Nacional de Desenvolvimento Científico e Tecnológico—Cnpq, Program Ciência sem Fronteiras—Doutorado Pleno no Exterior (GDE).

Data Availability Statement: The data presented in this study are openly available in University of Glasgow library at <http://theses.gla.ac.uk/> (accessed on 14 June 2021). For further information please contact D.M.d.A.F., A.E.G.S., or S.D.J.

Conflicts of Interest: The authors declare no conflict of interest.

References

1. Ventura, M.; Marinas, A.; Domine, M.E. Catalytic Processes for Biomass-Derived Platform Molecules Valorisation. *Top. Catal.* **2020**, *63*, 846–865. [CrossRef]
2. Liu, X.; Bouxin, F.P.; Fan, J.; Budarin, V.L.; Hu, C.; Clark, J.H. Recent Advances in the Catalytic Depolymerization of Lignin towards Phenolic Chemicals: A Review. *ChemSusChem* **2020**, *13*, 4296–4317. [CrossRef]
3. Crestini, C.; Lange, H.; Sette, M.; Argyropoulos, D.S. On the Structure of Softwood Kraft Lignin. *Green Chem.* **2017**, *19*, 4104–4121. [CrossRef]
4. Sjostrom, E. *Wood Chemistry: Fundamentals and Application*, 2nd ed.; Press, A., Ed.; Elsevier: Orlando, FL, USA, 1993. [CrossRef]
5. Abu-Omar, M.M.; Barta, K.; Beckham, G.T.; Luterbacher, J.S.; Ralph, J.; Rinaldi, R.; Román-Leshkov, Y.; Samec, J.S.M.; Sels, B.F.; Wang, F. Guidelines for Performing Lignin-First Biorefining. *Energy Environ. Sci.* **2021**, *14*, 262–292. [CrossRef]
6. Xu, C.; Arancon, R.A.D.; Labidi, J.; Luque, R. Lignin Depolymerisation Strategies: Towards Valuable Chemicals and Fuels. *Chem. Soc. Rev.* **2014**, *43*, 7485–7500. [CrossRef] [PubMed]
7. Pasquini, D.; Pimenta, M.T.B.; Ferreira, L.H.; Curvelo, A.A.D.S. Extraction of Lignin from Sugar Cane Bagasse and Pinus Taeda Wood Chips Using Ethanol-Water Mixtures and Carbon Dioxide at High Pressures. *J. Supercrit. Fluids* **2005**, *36*, 31–39. [CrossRef]
8. Melati, R.B.; Schmatz, A.A.; Pagnocca, F.; Contiero, J.; Brienza, M. Sugarcane Bagasse: Production, Composition, Properties, and Feedstock Potential. In *Sugarcane: Production Systems, Uses and Economic Importance*; Nova Science Publishers: Hauppauge, NY, USA, 2017; pp. 1–38.
9. Goldemberg, J.; Coelho, S.T.; Guardabassi, P. The Sustainability of Ethanol Production from Sugarcane. *Energy Policy* **2008**, *36*, 2086–2097. [CrossRef]
10. Pin, T.C.; Nascimento, V.M.; Costa, A.C.; Pu, Y.; Ragauskas, A.J.; Rabelo, S.C. Structural Characterization of Sugarcane Lignins Extracted from Different Protic Ionic Liquid Pretreatments. *Renew. Energy* **2020**, *161*, 579–592. [CrossRef]
11. Huijgen, W.J.J.; Reith, J.H.; Den Uil, H. Pretreatment and Fractionation of Wheat Straw by an Acetone-Based Organosolv Process. *Ind. Eng. Chem. Res.* **2010**, *49*, 10132–10140. [CrossRef]
12. Erdocia, X.; Prado, R.; Fernández-Rodríguez, J.; Labidi, J. Depolymerization of Different Organosolv Lignins in Supercritical Methanol, Ethanol, and Acetone to Produce Phenolic Monomers. *ACS Sustain. Chem. Eng.* **2016**, *4*, 1373–1380. [CrossRef]
13. Wu, Q.Y.; Ma, L.L.; Long, J.X.; Shu, R.Y.; Zhang, Q.; Wang, T.J.; Xu, Y. Depolymerization of Organosolv Lignin over Silica-Alumina Catalysts. *Chin. J. Chem. Phys.* **2016**, *29*, 474–480. [CrossRef]
14. Bauer, S.; Sorek, H.; Mitchell, V.D.; Ibáñez, A.B.; Wemmer, D.E. Characterization of Miscanthus Giganteus Lignin Isolated by Ethanol Organosolv Process under Reflux Condition. *J. Agric. Food Chem.* **2012**, *60*, 8203–8212. [CrossRef]
15. Lancefield, C.S.; Panovic, I.; Deuss, P.J.; Barta, K.; Westwood, N.J. Pre-Treatment of Lignocellulosic Feedstocks Using Biorenewable Alcohols: Towards Complete Biomass Valorisation. *Green Chem.* **2017**, *19*, 202–214. [CrossRef]
16. Bouxin, F.P.; McVeigh, A.; Tran, F.; Westwood, N.J.; Jarvis, M.C.; Jackson, S.D. Catalytic Depolymerisation of Isolated Lignins to Fine Chemicals Using a Pt/Alumina Catalyst: Part 1—Impact of the Lignin Structure. *Green Chem.* **2015**, *17*, 1235–1242. [CrossRef]
17. Lancefield, C.S.; Rashid, G.M.M.; Bouxin, F.; Wasak, A.; Tu, W.C.; Hallett, J.; Zein, S.; Rodríguez, J.; Jackson, S.D.; Westwood, N.J.; et al. Investigation of the Chemocatalytic and Biocatalytic Valorization of a Range of Different Lignin Preparations: The Importance of β -O-4 Content. *ACS Sustain. Chem. Eng.* **2016**, *4*, 6921–6930. [CrossRef]
18. McVeigh, A.; Bouxin, F.P.; Jarvis, M.C.; Jackson, S.D. Catalytic Depolymerisation of Isolated Lignin to Fine Chemicals: Part 2—Process Optimisation. *Catal. Sci. Technol.* **2016**, *6*, 4142–4150. [CrossRef]
19. Zhang, C.; Lu, J.; Zhang, X.; MacArthur, K.; Heggen, M.; Li, H.; Wang, F. Cleavage of the Lignin β -O-4 Ether Bond via a Dehydroxylation–Hydrogenation Strategy over a NiMo Sulfide Catalyst. *Green Chem.* **2016**, *18*, 6545–6555. [CrossRef]
20. Yamaguchi, A.; Mimura, N.; Shirai, M.; Sato, O. Bond Cleavage of Lignin Model Compounds into Aromatic Monomers Using Supported Metal Catalysts in Supercritical Water. *Sci. Rep.* **2017**, *7*, 1–7. [CrossRef] [PubMed]
21. Wang, X.; Rinaldi, R. Solvent Effects on the Hydrogenolysis of Diphenyl Ether with Raney Nickel and Their Implications for the Conversion of Lignin. *ChemSusChem* **2012**, *5*, 1455–1466. [CrossRef] [PubMed]
22. Li, J.; Sun, H.; Liu, J.-X.; Zhang, J.-j.; Li, Z.-X.; Fu, Y. Selective Reductive Cleavage of C–O Bond in Lignin Model Compounds over Nitrogen-Doped Carbon-Supported Iron Catalysts. *Mol. Catal.* **2018**, *452*, 36–45. [CrossRef]
23. Song, Q.; Wang, F.; Cai, J.; Wang, Y.; Zhang, J.; Yu, W.; Xu, J. Lignin Depolymerization (LDP) in Alcohol over Nickel-Based Catalysts via a Fragmentation–Hydrogenolysis Process. *Energy Environ. Sci.* **2013**, *6*, 994–1007. [CrossRef]
24. Baral, N.R.; Slutzky, L.; Shah, A.; Ezeji, T.C.; Cornish, K.; Christy, A. Acetone-Butanol-Ethanol Fermentation of Corn Stover: Current Production Methods, Economic Viability and Commercial Use. *FEMS Microbiol. Lett.* **2016**, *363*, 1–11. [CrossRef] [PubMed]
25. Gelder, E.A. The Hydrogenation of Nitrobenzene of Metal Catalysts. Ph.D. Thesis, The University of Glasgow, Glasgow, UK, 2005.

26. Munick de Albuquerque Fragoso, D.; Bouxin, F.P.; Montgomery, J.R.D.; Westwood, N.J.; Jackson, S.D. Catalytic Depolymerisation of Isolated Lignin to Fine Chemicals: Depolymerisation of Kraft Lignin. *Bioresour. Technol. Rep.* **2020**, *9*, 100400. [[CrossRef](#)]
27. McVeigh, A. The Conversion of Lignin to Alkylphenolic Monomers Using Heterogeneous Catalysis. Ph.D. Thesis, The University of Glasgow, Glasgow, UK, 2016.
28. Sarkanen, K.; Schuerch, C. Lignin Structure. XI: A Quantitative Study of the Alcoholysis of Lignin. *J. Am. Chem. Soc.* **1957**, *79*, 4203–4209. [[CrossRef](#)]
29. Danielle Munick de Albuquerque Fragoso. Lignin Conversion to Fine Chemicals. Ph.D. Thesis, University of Glasgow, Glasgow, UK, 2018.
30. Ekielski, A.; Mishra, P.K. Lignin for Bioeconomy: The Present and Future Role of Technical Lignin. *Int. J. Mol. Sci.* **2020**, *22*, 63. [[CrossRef](#)] [[PubMed](#)]
31. Huang, X.; Korányi, T.I.; Boot, M.D.; Hensen, E.J.M. Catalytic Depolymerization of Lignin in Supercritical Ethanol. *ChemSusChem* **2014**, *7*, 2276–2288. [[CrossRef](#)]
32. Nguyen, T.D.H.; Maschietti, M.; Belkheiri, T.; Amand, L.E.; Theliander, H.; Vamling, L.; Olausson, L.; Andersson, S.-I. Catalytic Depolymerisation and Conversion of Kraft Lignin into Liquid Products Using Near-Critical Water. *J. Supercrit. Fluids* **2014**, *86*, 67–75. [[CrossRef](#)]
33. Kawamata, Y.; Ishimaru, H.; Yamaguchi, K.; Yoshikawa, T.; Koyama, Y.; Nakasaka, Y.; Sato, S.; Masuda, T. Catalytic Cracking of Lignin Model Compounds and Degraded Lignin Dissolved in Inert Solvent over Mixed Catalyst of Iron Oxide and MFI Zeolite for Phenol Recovery. *Fuel Process. Technol.* **2020**, *197*, 106190. [[CrossRef](#)]
34. Mostafa, M.R.; Youssef, A.M.; Hassan, S.M. Conversion of Ethanol and Isopropanol on Alumina, Titania and Alumina-Titania Catalysts. *Mater. Lett.* **1991**, *12*, 207–213. [[CrossRef](#)]
35. Pillait, E.F.N.; Jain, R.A.I.; June, R.; Process, H. Catalytic Dehydration of Alcohols over Alumina: Mechanism of Ether Formation. *J. Catal.* **1967**, *9*, 322–330. [[CrossRef](#)]
36. Knözinger, H.; Ratnasamy, P. Catalytic Aluminas: Surface Models and Characterization of Surface Sites. *Catal. Rev.* **1978**, *17*, 31–70. [[CrossRef](#)]
37. Panov, A.G.; Fripiat, J.J. Acetone Condensation Reaction on Acid Catalysts. *J. Catal.* **1998**, *178*, 188–197. [[CrossRef](#)]
38. Varma, R.S.; Kabalka, G.W.; Evans, L.T.; Pagni, R.M. Aldol Condensations on Basic Alumina: The Facile Syntheses of Chalcones and Enones in a Solvent-Free Medium. *Synth. Commun.* **1985**, *15*, 279–284. [[CrossRef](#)]
39. NIST Chemistry WebBook. Acetone. Available online: <https://webbook.nist.gov/cgi/cbook.cgi?ID=C67641&Mask=4> (accessed on 14 July 2018).
40. Joffres, B.; Laurenti, D.; Charon, N.; Daudin, A.; Quignard, A.; Geantet, C. Thermochemical Conversion of Lignin for Fuels and Chemicals: A Review. *Oil Gas Sci. Technol. Rev. IFP Energ. Nouv.* **2013**, *68*, 753–763. [[CrossRef](#)]
41. Bouxin, F.P.; Zhang, X.; Kings, I.N.; Lee, A.F.; Simmons, M.J.H.; Wilson, K.; Jackson, S.D. Deactivation Study of the Hydrodeoxygenation of P-Methylguaiacol over Silica Supported Rhodium and Platinum Catalysts. *Appl. Catal. A Gen.* **2017**, *539*, 29–37. [[CrossRef](#)]
42. Hita, I.; Deuss, P.J.; Bonura, G.; Frusteri, F.; Heeres, H.J. Biobased Chemicals from the Catalytic Depolymerization of Kraft Lignin Using Supported Noble Metal-Based Catalysts. *Fuel Process. Technol.* **2018**, *179*, 143–153. [[CrossRef](#)]
43. Cheng, C.; Shen, D.; Gu, S.; Luo, K.H. State-of-the-Art Catalytic Hydrogenolysis of Lignin for the Production of Aromatic Chemicals. *Catal. Sci. Technol.* **2018**, *8*, 6275–6296. [[CrossRef](#)]
44. Chatterjee, M.; Chatterjee, A.; Ishizaka, T.; Kawanami, H. Rhodium-Mediated Hydrogenolysis/Hydrolysis of the Aryl Ether Bond in Supercritical Carbon Dioxide/Water: An Experimental and Theoretical Approach. *Catal. Sci. Technol.* **2015**, *5*, 1532–1539. [[CrossRef](#)]
45. He, J.; Lu, L.; Zhao, C.; Mei, D.; Lercher, J.A. Mechanisms of Catalytic Cleavage of Benzyl Phenyl Ether in Aqueous and Apolar Phases. *J. Catal.* **2014**, *311*, 41–51. [[CrossRef](#)]
46. He, J.; Zhao, C.; Mei, D.; Lercher, J.A. Mechanisms of Selective Cleavage of C-O Bonds in Di-Aryl Ethers in Aqueous Phase. *J. Catal.* **2014**, *309*, 280–290. [[CrossRef](#)]
47. Yoshikawa, T.; Shinohara, S.; Yagi, T.; Ryumon, N.; Nakasaka, Y.; Tago, T.; Masuda, T. Production of Phenols from Lignin-Derived Slurry Liquid Using Iron Oxide Catalyst. *Appl. Catal. B Environ.* **2014**, *146*, 289–297. [[CrossRef](#)]
48. Wang, S.; Zhang, K.; Li, H.; Xiao, L.-P.; Song, G. Selective Hydrogenolysis of Catechyl Lignin into Propenylcatechol over an Atomically Dispersed Ruthenium Catalyst. *Nat. Commun.* **2021**, *12*, 416. [[CrossRef](#)] [[PubMed](#)]
49. Lapiere, C.; Pollet, B.; Rolando, C. New Insights into the Molecular Architecture of Hardwood Lignins by Chemical Degradative Methods. *Res. Chem. Intermed.* **1995**, *21*, 397–412. [[CrossRef](#)]
50. Kang, S.; Li, X.; Fan, J.; Chang, J. Hydrothermal Conversion of Lignin: A Review. *Renew. Sustain. Energy Rev.* **2013**, *27*, 546–558. [[CrossRef](#)]
51. Yuan, Z.; Tymchyshyn, M.; Xu, C. Reductive Depolymerization of Kraft and Organosolv Lignin in Supercritical Acetone for Chemicals and Materials. *ChemCatChem* **2016**, *8*, 1968–1976. [[CrossRef](#)]
52. Fang, Z.; Sato, T.; Smith, R.L.; Inomata, H.; Arai, K.; Kozinski, J.A. Reaction Chemistry and Phase Behavior of Lignin in High-Temperature and Supercritical Water. *Bioresour. Technol.* **2008**, *99*, 3424–3430. [[CrossRef](#)]
53. Ravenelle, R.M.; Copeland, J.R.; Kim, W.-G.; Crittenden, J.C.; Sievers, C. Structural Changes of γ -Al₂O₃-Supported Catalysts in Hot Liquid Water. *ACS Catal.* **2011**, *1*, 552–561. [[CrossRef](#)]

-
54. Sattler, J.J.H.B.; Beale, A.M.; Weckhuysen, B.M. Operando Raman Spectroscopy Study on the Deactivation of Pt/Al₂O₃ and Pt-Sn/Al₂O₃ Propane Dehydrogenation Catalysts. *Phys. Chem. Chem. Phys.* **2013**, *15*, 12095. [[CrossRef](#)]
 55. Sadezky, A.; Muckenhuber, H.; Grothe, H.; Niessner, R.; Pöschl, U. Raman Microspectroscopy of Soot and Related Carbonaceous Materials: Spectral Analysis and Structural Information. *Carbon* **2005**, *43*, 1731–1742. [[CrossRef](#)]